Title
RESONANCE PRODUCTION IN n+p INTERACTIONS BETWEEN 3 AND 4 GeV/c

Authors
Gidal, G.
Brown, D.
Birge, R.W.
et al.

Publication Date
1967-12-26

University of California

Ernest O. Lawrence Radiation Laboratory

RESONANCE PRODUCTION IN π^+p INTERACTIONS
BETWEEN 3 AND 4 GeV/c

G. Gidal, D. Brown, R. W. Birge, R. Bacastow,
S. Y. Fung, W. Jackson, and R. T. Pu

December 26, 1967

DISCLAIMER

For Proceedings of Third Topical Conference on Resonant Particles, Athens, Ohio, November 22-24, 1967

UCRL-17984
Preprint

UNIVERSITY OF CALIFORNIA

Lawrence Radiation Laboratory
Berkeley, California

AEC Contract No. W-7405-eng-48

RESONANCE PRODUCTION IN π^+p INTERACTIONS BETWEEN 3 AND 4 GeV/c

G. Gidal, D. Brown, R. W. Birge, R. Bacastow, S. Y. Fung, W. Jackson, and R. T. Pu

December 26, 1967

RESONANCE PRODUCTION IN π^+p INTERACTIONS BETWEEN 3 and 4 GeV/c*

G. Gidal, D. Brown, and R. W. Birge

Lawrence Radiation Laboratory
University of California
Berkeley, California

and

R. Bacastow, S. Y. Fung, W. Jackson, and R. T. Pu

University of California
Riverside, California

December 26, 1967

We report on two experiments from an exposure of the 72-inch H_2 bubble chamber to π^+ mesons at the five momenta 2.95, 3.2, 3.5, 3.75, and 4.1 GeV/c:

(A) observation of the B enhancement, using 9400 events of the type

$$\pi^+p \rightarrow \pi^+p\pi^+\pi^-\pi^\circ; \qquad (1)$$

(B) the decay of N^* resonances into $\Delta^{++}\pi^-$, using 7800 events of the type

$$\pi^+p \rightarrow \pi^+p\pi^+\pi^-. \qquad (2)$$

(A) Since the B enhancement in the $\omega\pi$ system was discovered in π^+p interactions[1] it has been an enigma. The enhancement was confirmed in other π^+p experiments,[2] but Goldhaber et al.[3] observed that the outer region of the ω Dalitz plot contributed much more heavily to the B meson than the inner region. Chung et al.[4] observed the B in π^+p collisions between 3 and 4 GeV/c and gave arguments for its being a kinematic effect. In particular, they observed that the B peak came from events with small momentum transfer to high-mass π^-p systems, events in which the outgoing proton went forward in the π^-p center of mass, contributing heavily. They then concluded that a combination of the processes $pp \rightarrow \pi p$ and isobar production could give such an effect, and that the B enhancement was probably a kinematic reflection of these processes. They realized, however, that one could not rule out a reversal of this argument. Subsequently, Baltay et al.[5] observed the B meson in $\bar{p}p$ annihilations at rest in the reaction $\bar{p}p \rightarrow \omega^\circ\pi^+\pi^-$, a process in which the kinematic effects discussed above cannot exist. No evidence of the anomaly in the Dalitz plot reported by Goldhaber et al. was observed in either the π^-p or $\bar{p}p$ experiments.

In reaction (1), 3250 events with $0.75 < M(\pi^+\pi^-\pi^\circ) < 0.82$ were assigned to the reaction $\pi^+p \rightarrow \pi^+p\omega^\circ$. The $\omega\pi$ mass spectrum is presented in Fig. 1, showing the B enhancement of about 150 events above background near 1230 MeV. Requiring no Δ^{++} in the π^+p system or limiting momentum transfer to the proton to less than -1.0 GeV/c^2 each preserves a large part of the enhancement, indicating that here, too, the B is primarily associated with higher-mass πp systems and the lower momentum transfers. Double ω° events are seen not to contribute significantly to the B peak, and are included in all graphs with a weight of 1/2 for each combination. The solid curve is phase space. A model which assumes that the dominant reaction is $\omega^\circ\Delta^{++}$ with production angular distribution e^{3t_Δ} is shown as the dotted curve. We see that the background for all events with an ω° is relatively flat in the B region; the background after cuts is considerably more model-dependent.

Figure 2 shows the same curve for events in which the 3π system lies only in the nearby mass band 0.82 to 1.0 GeV. No B enhancement is seen. To compare this experiment with that of Chung et al. we show in Fig. 3 the πp mass spectra produced with the ω°. Whereas the $\pi^{-}p$ spectrum shows the copious production of higher-mass isobars, the $\pi^{+}p$ spectrum is completely dominated by the $\Delta^{++}(1238)$, higher-mass $I = 3/2$ isobars not being produced at most of our energies. What is important to note is that the isobar production is very different for the two experiments.

Figure 4 shows the angular distribution of the outgoing proton with respect to the incident proton in the πp center of mass, for several πp mass intervals. As noted by Chung et al., the Δ^{++} region shows the characteristic $\cos^{2}\theta$ component and the higher-mass regions show a forward peak increasing in amplitude with increasing πp mass. The shaded region in the $\pi^{-}p$ case is their estimate of the events contributing to the B peak from each mass region. The shaded region in the $\pi^{+}p$ case is produced by inverting the argument, i.e., we assume production of the $\pi^{+}\omega^{\circ}p$ system according to phase space $\times$ $e^{3t}p$. A Monte Carlo calculation of such events then produces the shaded $\cos\theta pp$ distributions. In Fig. 5 we show the same comparison, restricting the $\pi^{+}\omega^{\circ}$ mass to lie in the B region (1.1 to 1.3 GeV). The shaded region is normalized to the 150 B events estimated from Fig. 1, and is seen to account for the forward peaking. Although the reaction $\rho p \rightarrow \pi p$ is expected to produce a forward peaking at high πp masses, no explicit model that also produces a B enhancement has been exhibited.

In Figure 6 we show our attempt to determine the production cross sections for the reactions $\pi^{+}p \rightarrow B^{+}p$ in the momentum range 3 to 4 GeV/c. Whenever possible we have combined our data with other available samples to increase the statistics. It is very difficult to estimate the background. The solid curves are 60% phase space, + 40% reflection of the dominant

$\Delta^{++}\omega^{\circ}$ process assuming an $e^{3t_{\Delta}}$ production angular distribution and isotropic decay distribution. Crude estimates give the following values for the B-meson production cross sections. This experiment alone gives an average cross section of 0.06 mb, slightly lower than the "world average" of 0.076 mb.

P_{π^+} (GeV/c)	Events/mb	Estimated Number of B events	σ (mb)
2.95 + 3.2	1000	65	0.065 ± 0.03
3.5	1208	110	0.091 ± 0.025
3.75	1025	75	0.073 ± 0.025
4.05	1080	80	0.074 ± 0.030

We have separately looked at the $\omega^{\circ}\pi^{+}$ mass distribution for the two regions of the ω° Dalitz plot[3] and see no significant difference in the B signal for the two regions. The results are shown in Fig. 7. As expected, the background increases considerably in the outer region.

(B) We would like to present evidence for the "cascade" decay of higher N^{*}s into $\Delta^{++}\pi^{-}$. Events from reaction (2) were selected with $\Delta^{++}\left[1.12 < M(\pi^{+}p) \leq 1.32 \text{ GeV}\right]$, no ρ° $\left[0.68 < M(\pi^{+}\pi^{-}) < 0.84 \text{ GeV}\right]$, $t_p > 0.1\ \text{GeV}/c^2$, and $t_{\Delta^{++}} > 0.3\ \text{GeV}/c^2$. The last two requirements were used to eliminate the tail of the more dominant $A^{+}p$ and $\Delta^{++}\rho^{\circ}$ reactions. The resulting distribution of $M(\Delta^{++}\pi^{-})$ for all events among the five energies is shown in Figure 8. For a simple fit, we assume five resonances of the Breit-Wigner form plus a background. The ordinary phase space (PS) is allowed to be modified by a linear function of the $(\Delta^{++}\pi^{-})$ Energy E. Thus the fitted curve has the form

$$\left(\sum_{i=1}^{5} F_i B_i + F_B\right) \left(1 - C E\right) PS,$$

$$B_i = \frac{\Gamma_i^2/4}{(M_i - E)^2 + \Gamma_i^2/4}$$

and yields the following parameters

i	M_i (MeV)	Γ_i (MeV)	F_i
1	1520	242	2.37
2	1665	98	1.49
3	1926	156	0.37
4	2193	114	0.55
5	2388	51	0.46
$F_B = 0.56$; $C = 0.047$			

The fitted background (dashed curve) is only slightly modified from the ordinary phase space ($C = 0.047$, and hence negligible). The background from the reflection of the $\Delta^{++}\rho^{\circ}$ final state, remaining after the cuts, would peak toward the higher mass values and so does not contribute to the peaking around 1.6. In view of yesterday's discussions it is perhaps interesting to point out that the events removed with the $t_{\Delta^{++}}$ cut appear as a shoulder near $M(\Delta^{++}\pi^-) = 1450$ MeV produced with very small momentum transfer to the π^+. The known cluster of $I = 1/2$ and $I = 3/2$ resonances in the general region of 1.5 to 1.7 are roughly accounted for by the lowest two fitted resonances. Because the highest resonance can be produced only at the highest momenta, the fitted width is rather narrow. Over all, the positions of the fitted resonances as well as the width of the middle resonances are in good agreement with the known resonances in this energy region. Of course the resonance production varies with beam energy, and Figure 9 shows the $M(\Delta^{++}\pi^-)$ distributions for the three groups of incident momenta. We note that the N*(1920) is produced at the lower momenta whereas the N*(2190) is produced more at the higher momenta. Part of the latter is certainly a threshold effect, as is the onset of N*(2420) production at the highest momenta. One is tempted to attribute the disappearance of N*(1920) to the onset of N*(2850) in the direct channel, whose decay into the even-parity resonance N*(1920) + π^- might be suppressed relative to its decay into the odd-parity resonance N*(2190) + π^-. Figure 10 shows the production angular distributions for the three dominant regions of $\Delta^{++}\pi^-$ mass. As expected, both the 1660 and 1920 regions become more peripheral as the energy increases.

REFERENCES

*Work done under auspices of the U. S. Atomic Energy Commission.

1. M. Abolins, R. Lander, W. Melhop, W. Xuong, and P. Yager, Phys. Rev. Letters 11, 381 (1963); Proceedings Second Topical Conference on Resonant Particles (1965) - B. A. Munir, P. 198.

2. Aachen-Berlin-Birmingham-Bonn-Hamburg-London (I.C.)-Munich Collaboration, Phys. Rev. 138B 897 (1965).

3. G. Goldhaber, S. Goldhaber, J. Kadyk, and B. Shen, Phys. Rev. Letters 15, 118 (1965).

4. S. Chung, M. Neveu-Rene, O. Dahl, J. Kirz, D. Miller, and Z. Guiragossian, Phys. Rev. Letters 16, 481 (1966).

5. C. Baltay, J. Severiens, N. Yeh, and D. Zanello, Phys. Rev. Letters 18, 93 (1967).

FIGURE CAPTIONS

Fig. 1. $\omega\pi$ mass spectrum for reaction $\pi^+p \rightarrow \pi^+p\omega^\circ$: (a) all events (b) events with no Δ^{++}, (c) events with $t_p < -1.0$ GeV/c^2.

Fig. 2. 4π mass spectrum for events with 3π mass in "nearby" mass band, 0.82 to 1.0 GeV.

Fig. 3. πp mass spectra in reactions (a) $\pi^+p \rightarrow \pi^+p\omega^\circ$ and (b) $\pi^-p \rightarrow \pi^-p\omega^\circ$.

Fig. 4. Angular distribution of outgoing proton with respect to incident proton in πp center of mass for πp mass intervals indicated, in reactions (a) $\pi^+p \rightarrow \pi^+p\omega^\circ$ and (b) $\pi^-p \rightarrow \pi^-p\omega^\circ$. Shaded regions are explained in text.

Fig. 5. Angular distributions of outgoing proton with respect to incident proton in πp center of mass when $\pi\omega$ system is restricted to B region. Shaded regions are explained in text.

Fig. 6. $\omega\pi$ mass spectrum for reaction $\pi^+p \rightarrow \pi^+p\omega^\circ$ for four groups of incident π^+ momentum.

Fig. 7. Comparison of $\omega\pi$ mass distributions of "inner" and "outer" regions of ω Dalitz plot.

Fig. 8. $\Delta^{++}\pi^-$ mass distributions for all five momenta combined. Cuts and fitted curves are explained in text.

Fig. 9. $\Delta^{++}\pi^-$ mass distributions for three momentum intervals.

Fig. 10. Production angular distributions of dominant resonance regions.

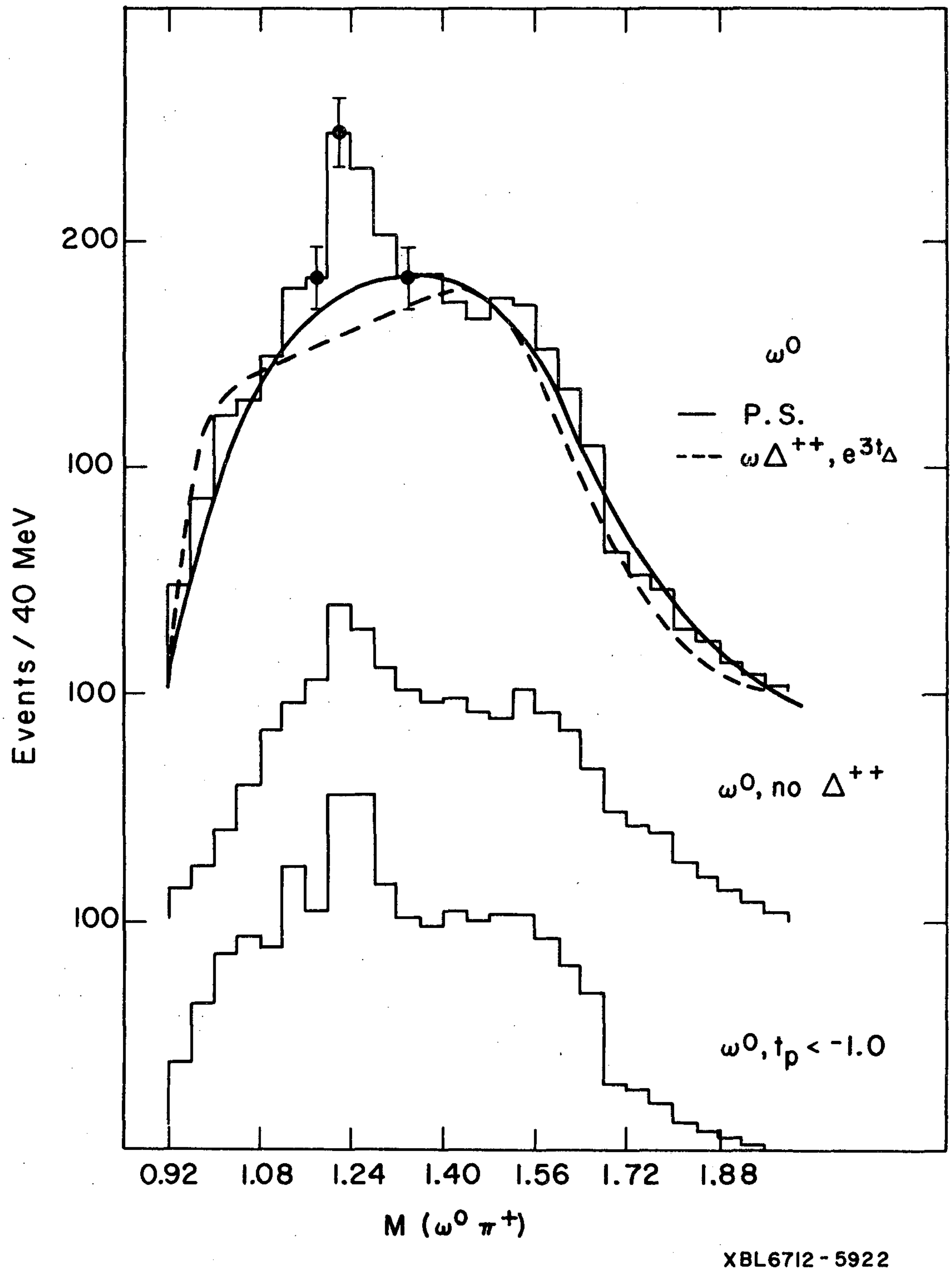
200
100
100
100
Events / 40 MeV
ω^0
— P. S.
--- $\omega\Delta^{++}, e^{3t_\Delta}$
ω^0, no Δ^{++}
$\omega^0, t_p < -1.0$
0.92
1.08
1.24
1.40
1.56
1.72
1.88
M ($\omega^0\pi^+$)
XBL6712-5922

Fig. 1

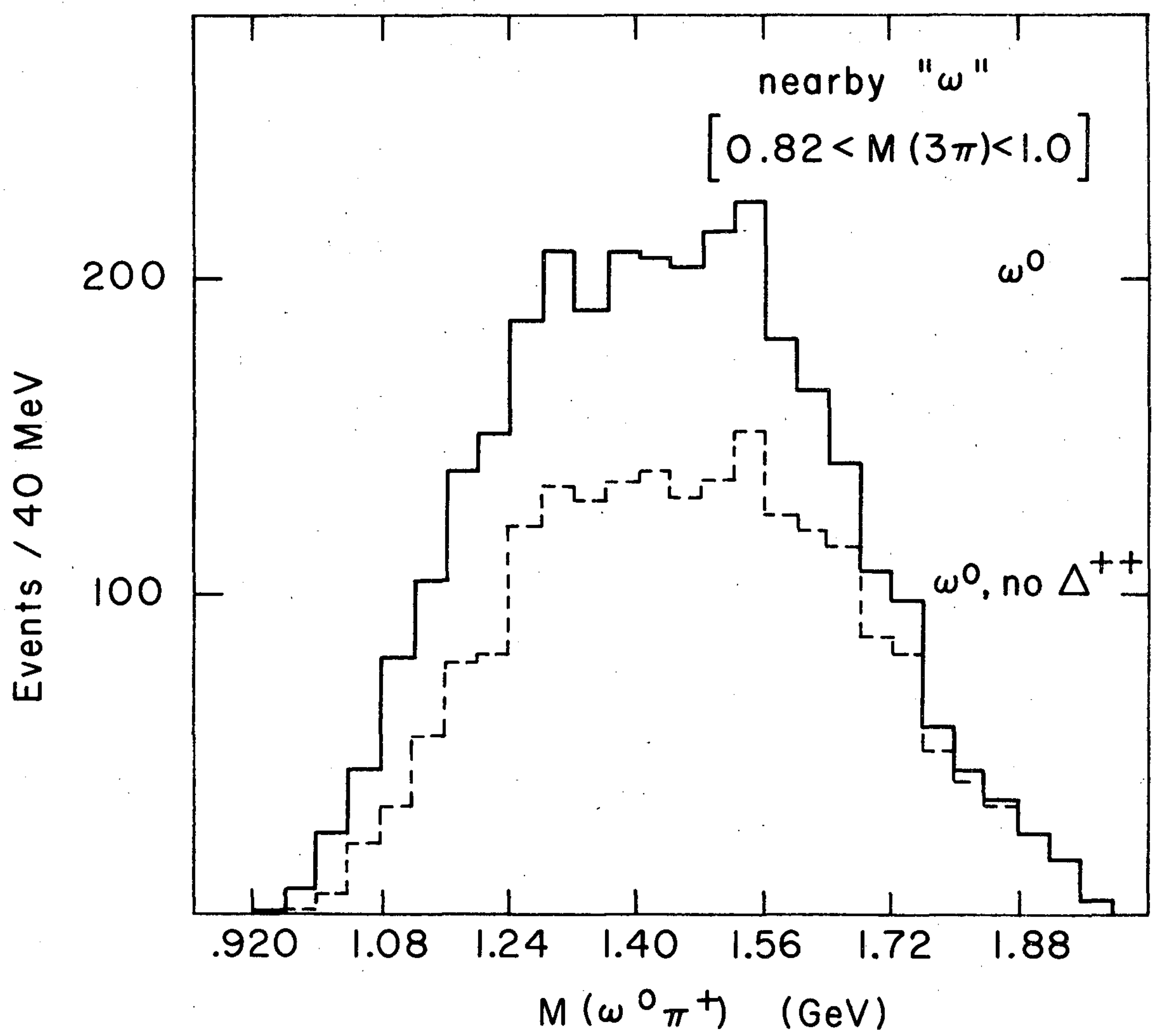

XBL 6712-5924

Fig. 2

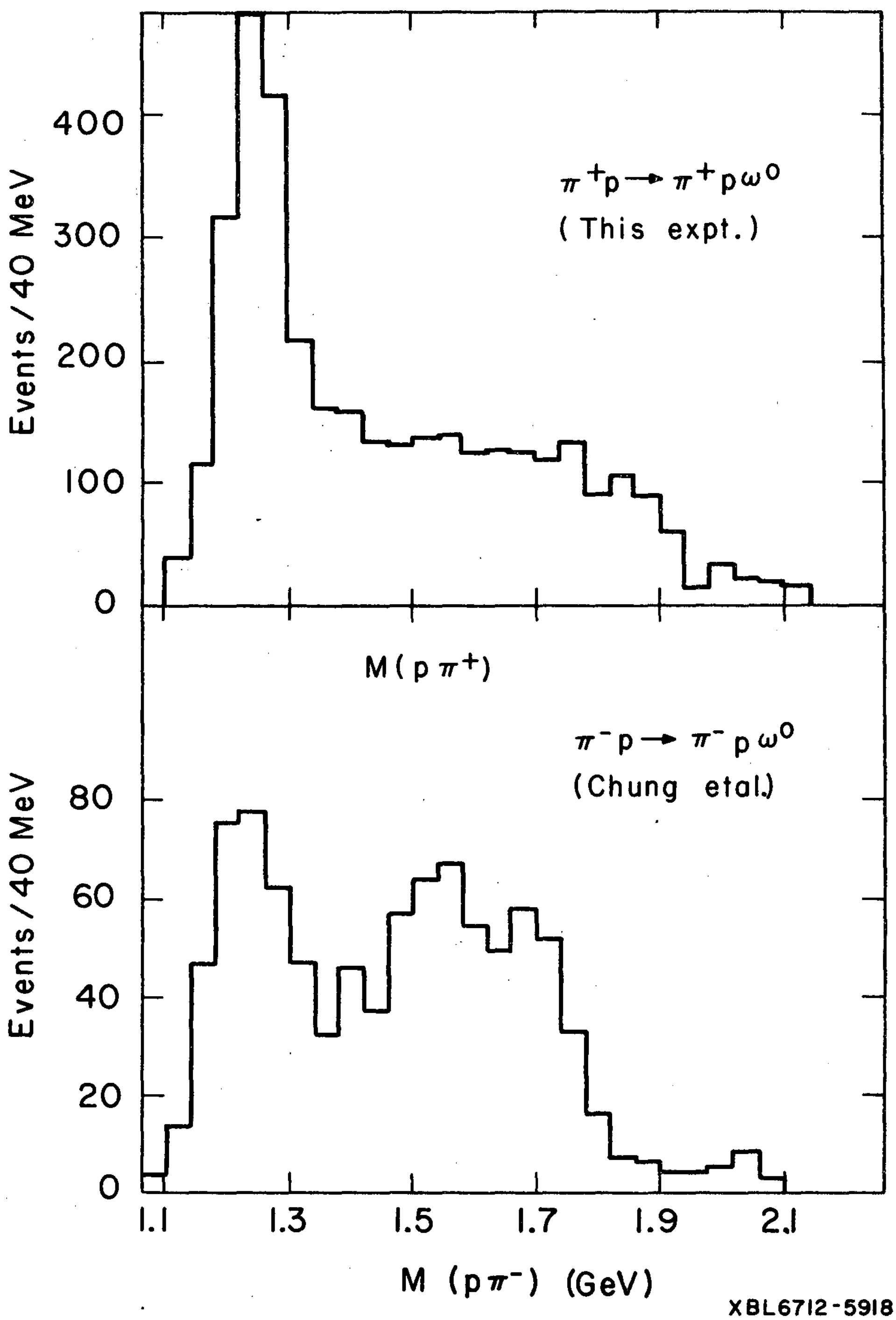
Events / 40 MeV
400
300
200
100
0
$\pi^+ p \to \pi^+ p \omega^0$
(This expt.)
M(p π^+)
$\pi^- p \to \pi^- p \omega^0$
(Chung etal.)
Events / 40 MeV
80
60
40
20
0
1.1
1.3
1.5
1.7
1.9
2.1
M (pπ^-) (GeV)
XBL6712-5918

Fig. 3

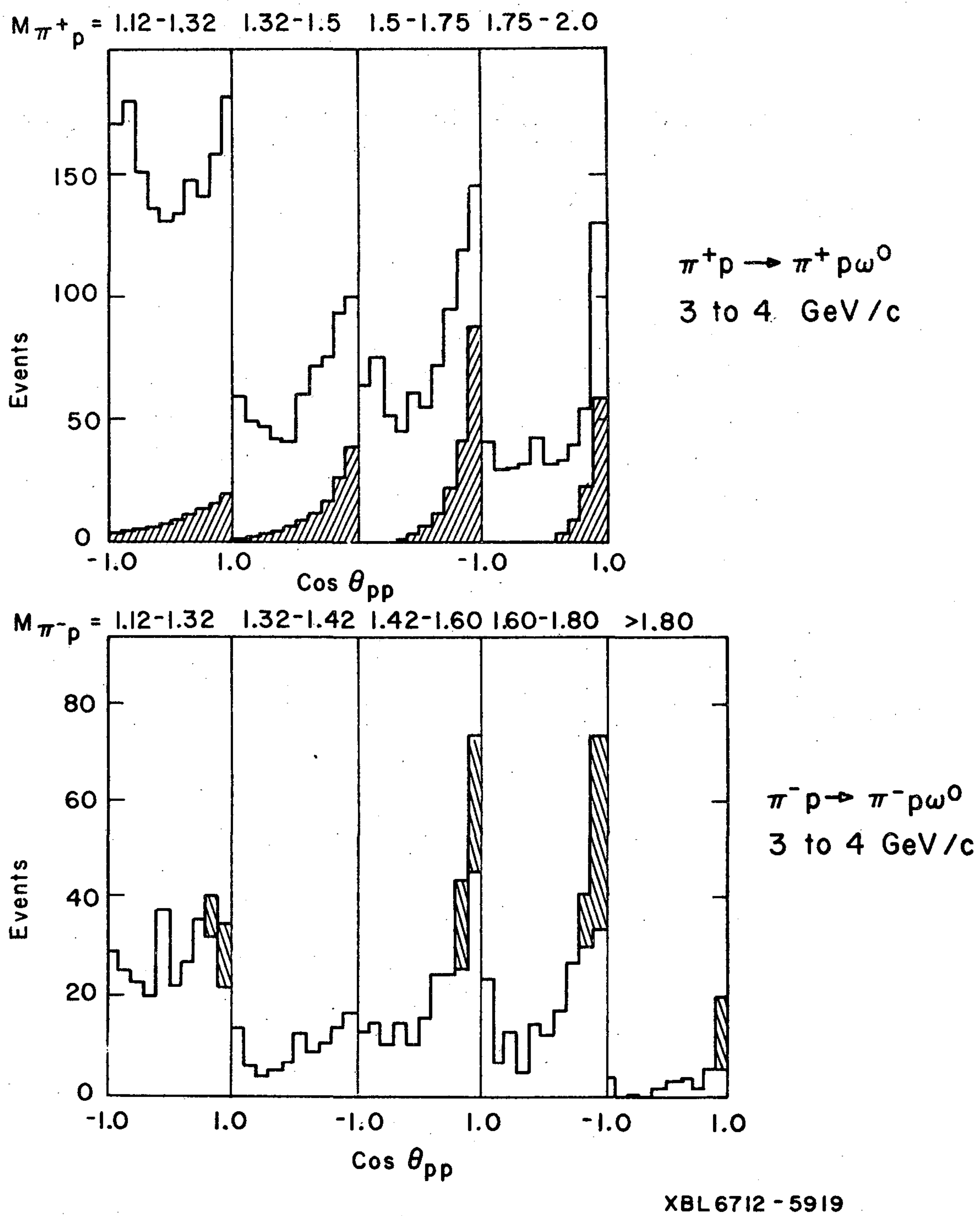
M_{π^+p} = 1.12-1.32 1.32-1.5 1.5-1.75 1.75-2.0
Events
150
100
50
0
-1.0
1.0
-1.0
1.0
Cos θ_{pp}
$\pi^+p \to \pi^+p\omega^0$
3 to 4 GeV/c
M_{π^-p} = 1.12-1.32 1.32-1.42 1.42-1.60 1.60-1.80 >1.80
Events
80
60
40
20
0
-1.0
1.0
-1.0
1.0
-1.0
1.0
Cos θ_{pp}
$\pi^-p \to \pi^-p\omega^0$
3 to 4 GeV/c
XBL 6712-5919

Fig. 4

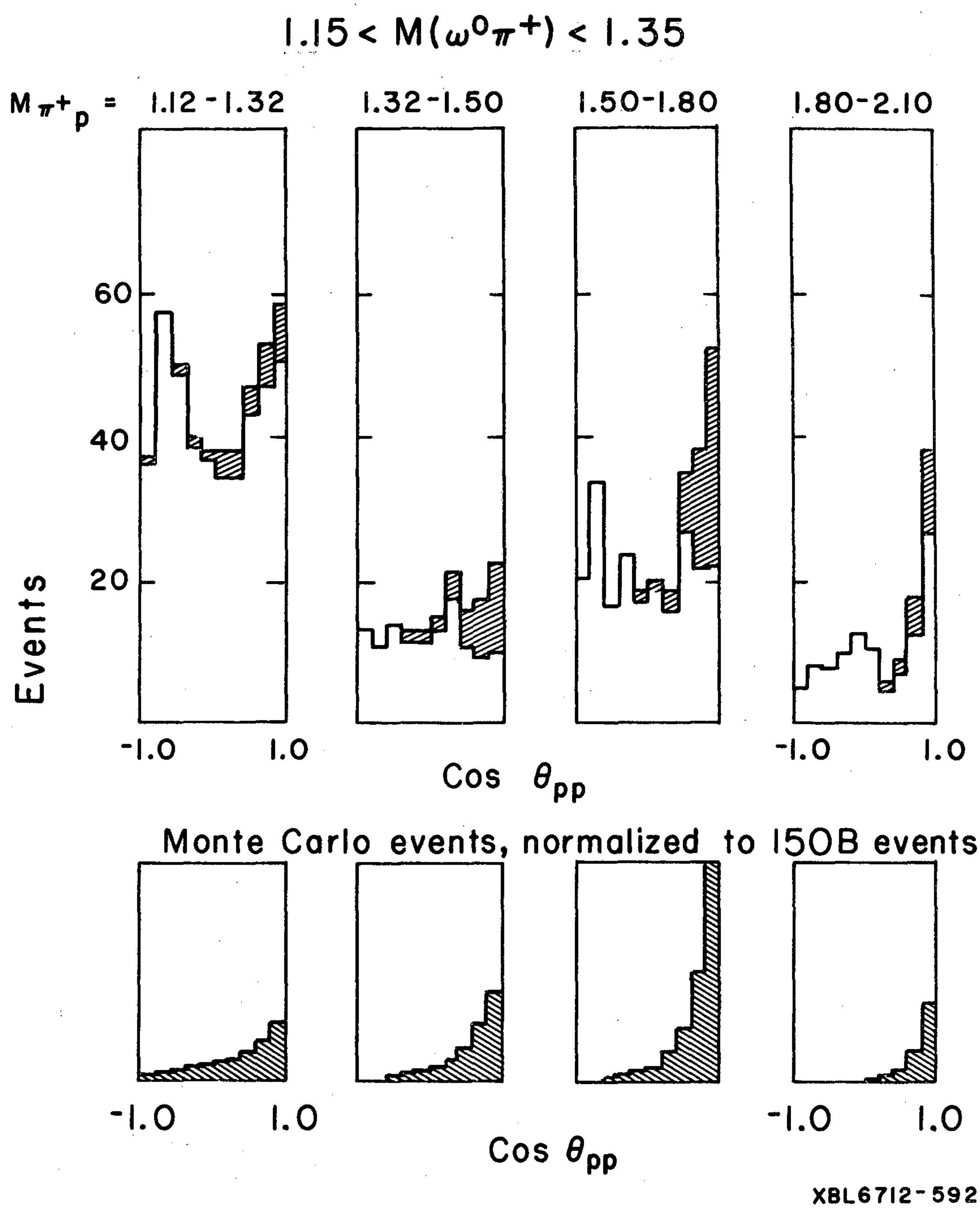
1.15 < M($\omega^0\pi^+$) < 1.35
M_{π^+p} = 1.12-1.32
1.32-1.50
1.50-1.80
1.80-2.10
60
40
20
Events
-1.0
1.0
Cos θ_{pp}
Monte Carlo events, normalized to 1508 events
-1.0
1.0
Cos θ_{pp}
XBL6712-5921

Fig. 5

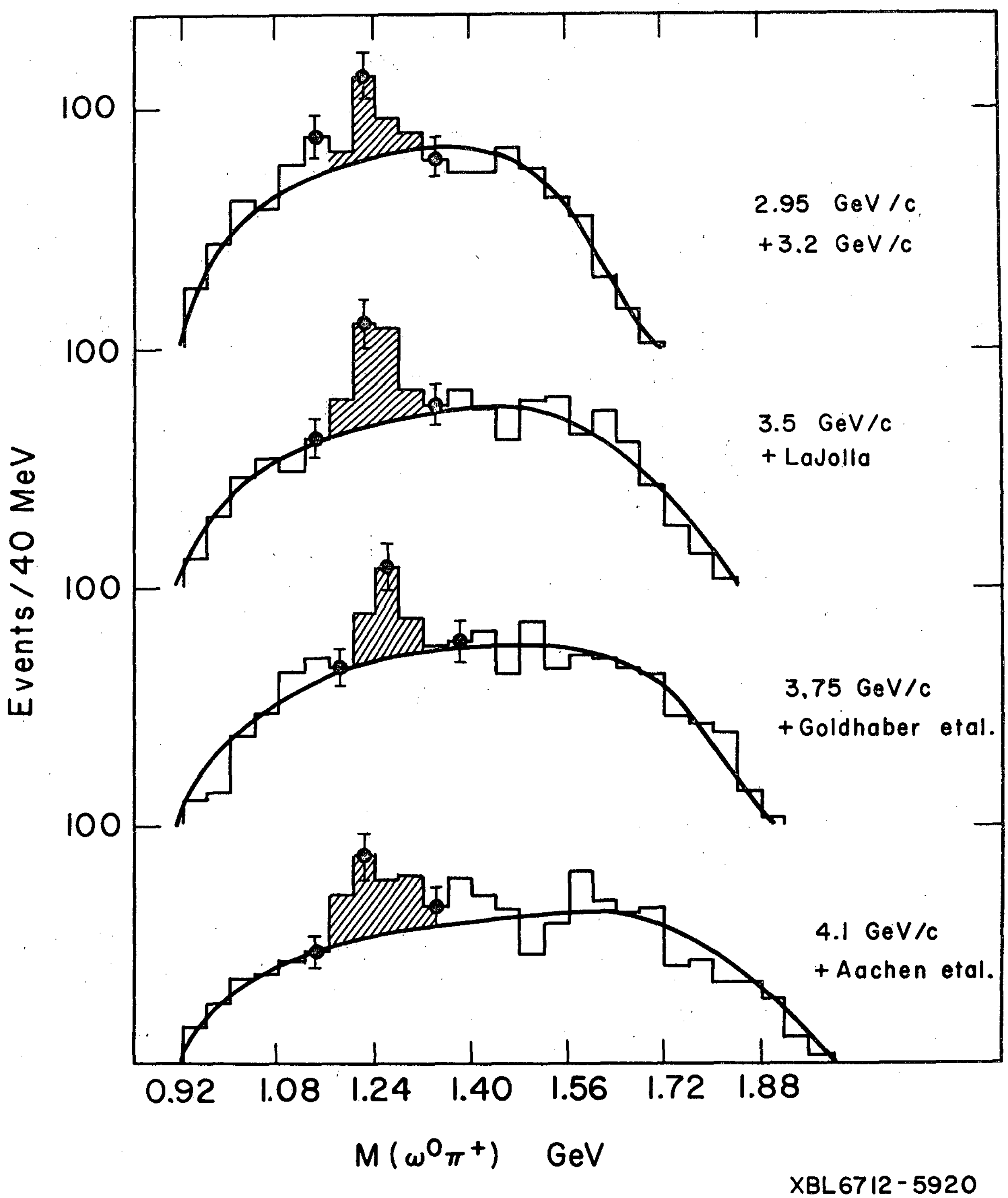
100
100
100
100
Events / 40 MeV
2.95 GeV/c
+3.2 GeV/c
3.5 GeV/c
+ LaJolla
3.75 GeV/c
+ Goldhaber etal.
4.1 GeV/c
+ Aachen etal.
0.92 1.08 1.24 1.40 1.56 1.72 1.88
M (ω⁰π⁺) GeV
XBL6712-5920

Fig. 6

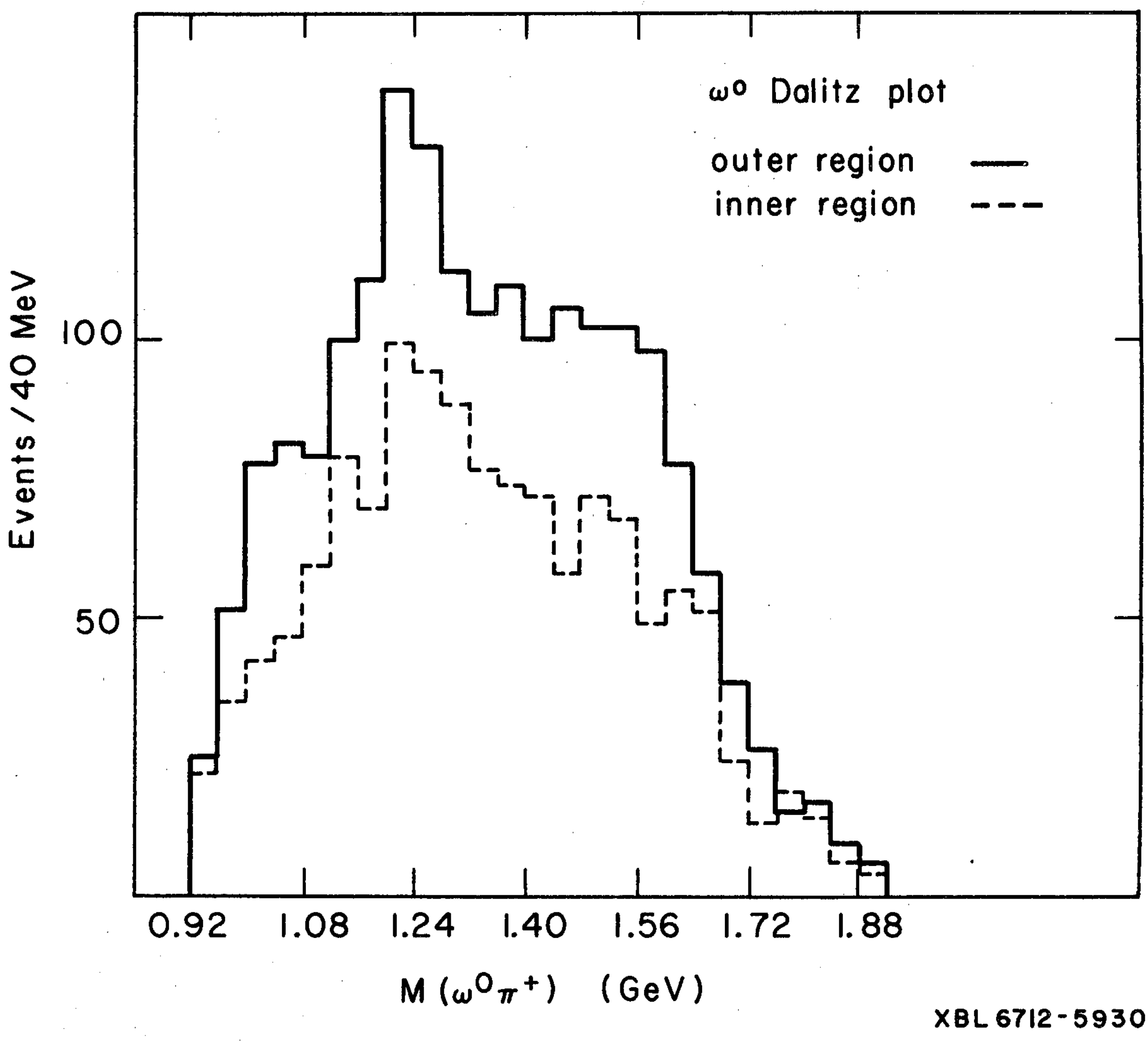
ω⁰ Dalitz plot
outer region
inner region
Events / 40 MeV
100
50
0.92
1.08
1.24
1.40
1.56
1.72
1.88
M (ω⁰π⁺) (GeV)
XBL 6712-5930

Fig. 7

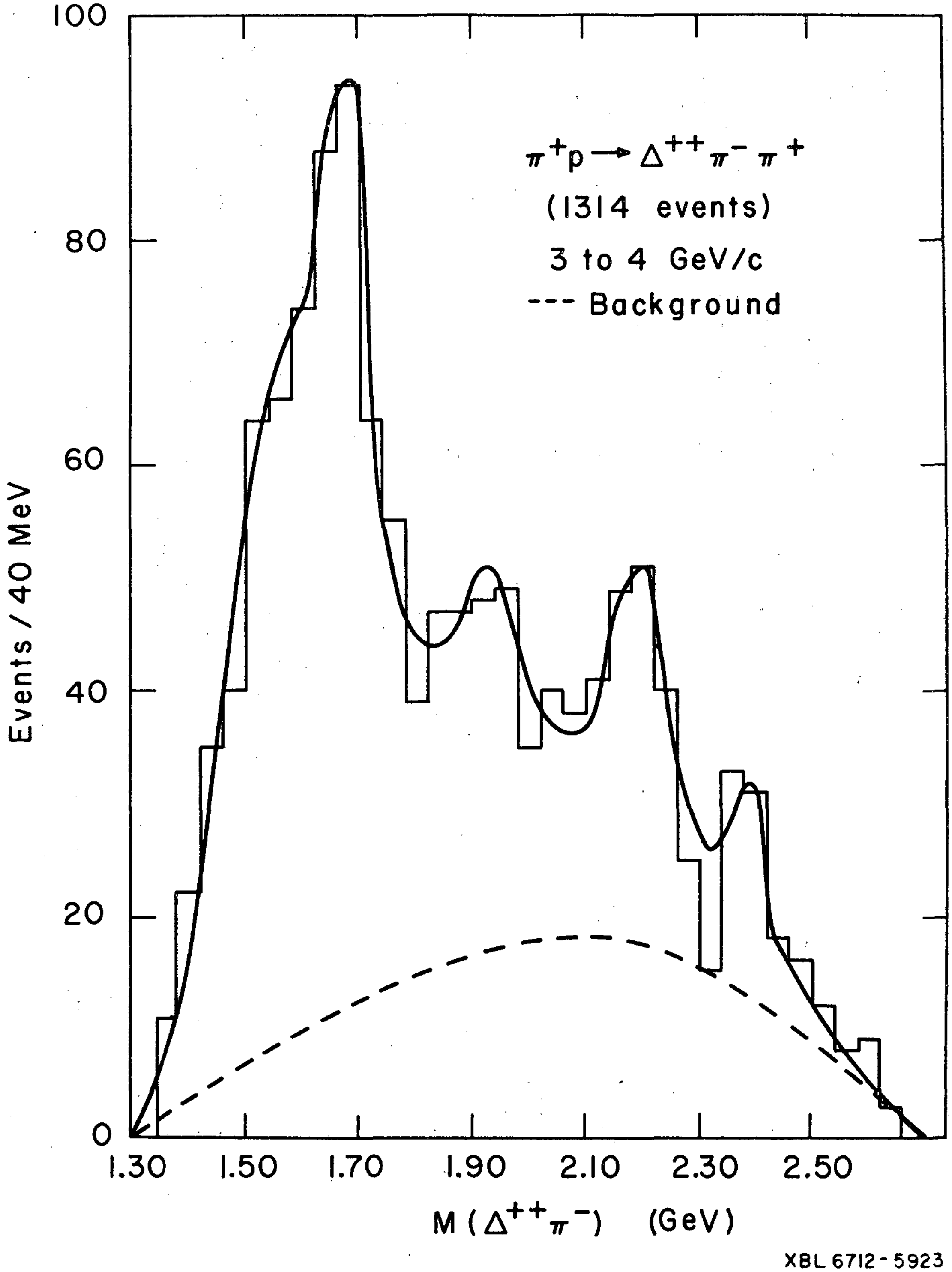

100
80
60
40
20
0
Events / 40 MeV
1.30
1.50
1.70
1.90
2.10
2.30
2.50
M (Δ++π−) (GeV)
π+p → Δ++π− π+
(1314 events)
3 to 4 GeV/c
--- Background
XBL 6712-5923

Fig. 8

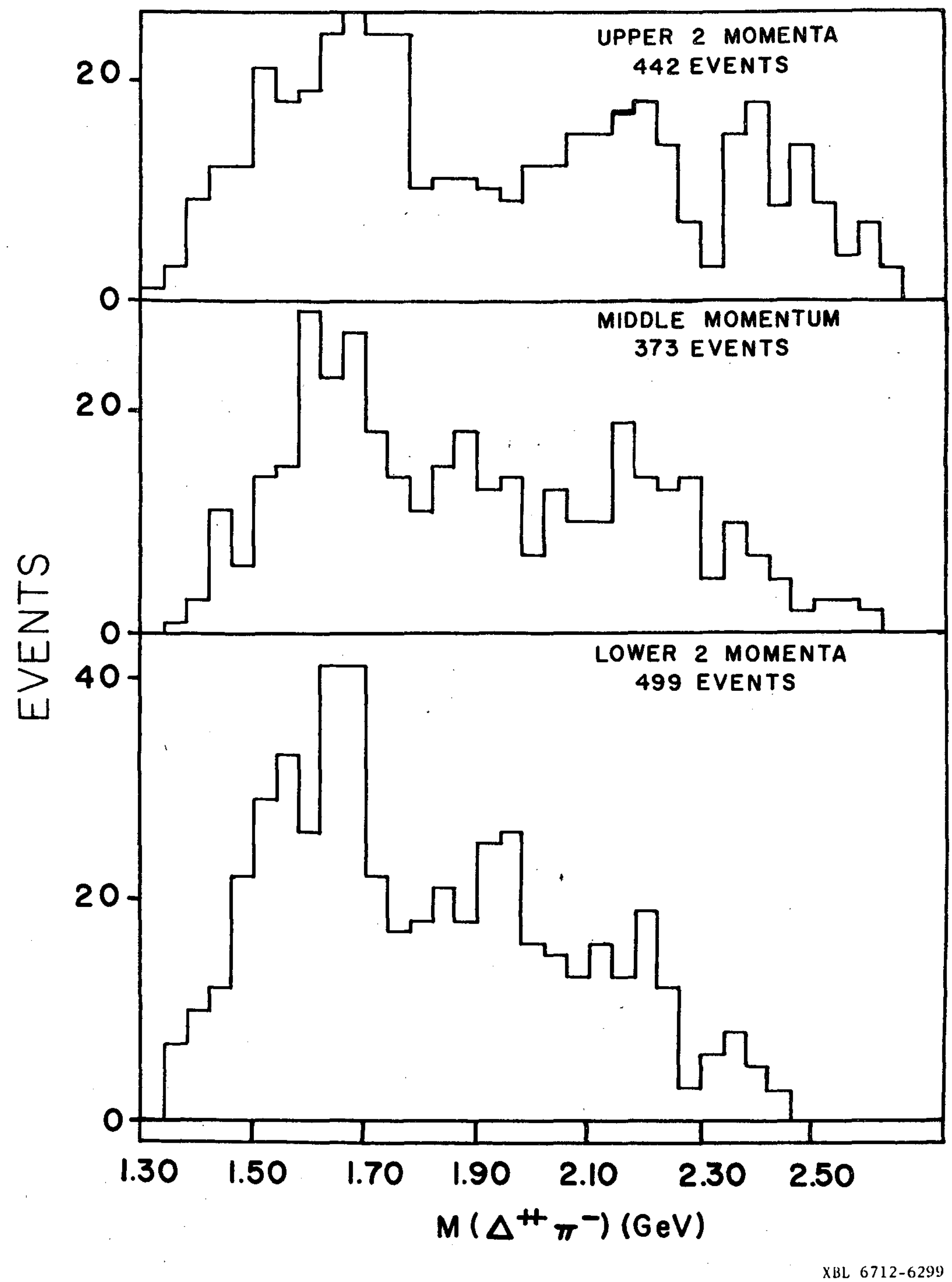
UPPER 2 MOMENTA
442 EVENTS
MIDDLE MOMENTUM
373 EVENTS
LOWER 2 MOMENTA
499 EVENTS
EVENTS
20
0
20
0
40
20
0
1.30
1.50
1.70
1.90
2.10
2.30
2.50
M (Δ++ π−) (GeV)
XBL 6712-6299

Fig. 9

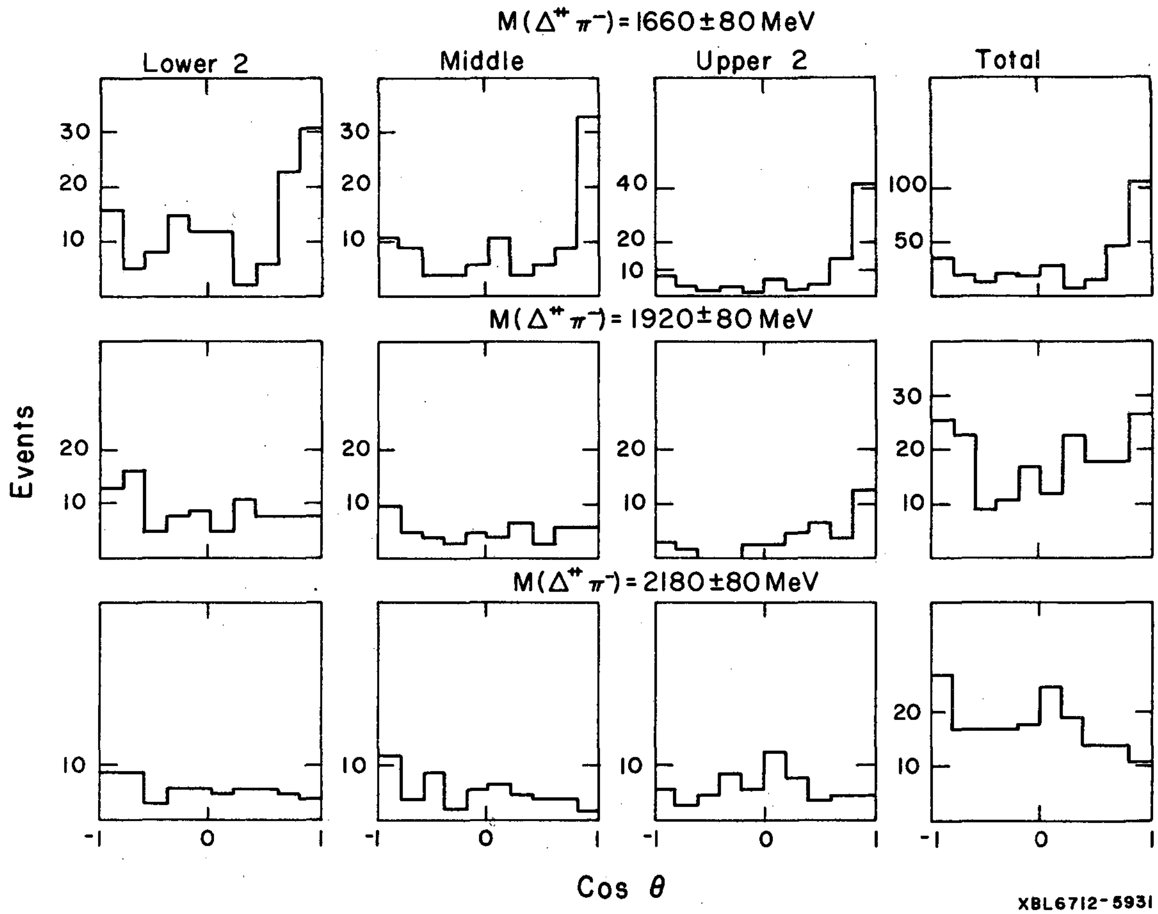

M(Δ⁺⁺ π⁻) = 1660 ± 80 MeV
Lower 2
Middle
Upper 2
Total
M(Δ⁺⁺ π⁻) = 1920 ± 80 MeV
M(Δ⁺⁺ π⁻) = 2180 ± 80 MeV
Events
Cos θ
XBL6712-5931

Fig. 10